COMPARISON OF TWO NONLINEAR FILTERING TECHNIQUES - THE EXTENDED KALMAN FILTER AND THE FEEDBACK PARTICLE FILTER

BY

KRISHNA KALYAN MEDARAMETLA

THESIS

Submitted in partial fulfillment of the requirements
for the degree of Master of Science in Mechanical Engineering
in the Graduate College of the
University of Illinois at Urbana-Champaign, 2014

Urbana, Illinois

Adviser:

Associate Professor Prashant Mehta

ABSTRACT

In a recent work it has been shown that importance sampling can be avoided in particle filter through an innovation structure inspired by traditional nonlinear filtering combined with optimal control and mean-field game formalisms. The resulting algorithm is referred to as feedback particle filter (FPF)

The purpose of this thesis is to provide a comparative study of the feedback particle filter (FPF) with the extended Kalman filter (EKF) for a scalar filtering problem which has linear signal dynamics and nonlinear observation dynamics. Different parameters of the signal model and observation model will be varied and performance of the two filtering techniques FPF, EKF will be compared.

To my family, friends, and professors

ACKNOWLEDGMENTS

I would like to express my sincere gratitude to my advisor Professor Prashant Mehta for giving me the opportunity to work on this thesis and several other challenging problems over the course of the last one year, for his assistance in the preparation of this manuscript and for all his constant guidance and support. I have thoroughly enjoyed my time working with him and have learnt a lot from him.

I would like to thank my friends for their constant support. Last but not the least I would like to thank my family, for their unconditional love and incredible patience

TABLE OF CONTENTS

LIST OF ABBREVIATIONS

EKF	Extended Kalman Filter
FPF	Feedback Particle Filter
EL-BVP	Euler-Lagrange Boundary Value Problem

CHAPTER 1

INTRODUCTION

Filtering is an area which originated from the simple problems of tracking and signal processing but the underlying principle is very general and is ubiquitous in modern day applied problems such as global positioning systems (GPS), robotics and climate prediction, where increasingly stochastic processes are being used to model complex dynamic phenomenon.

A filtering problem usually consists of estimating an unknown dynamic state of a stochastic system based on a set of noisy observations of the same. This basic problem is encountered in many fields including but not limited to target tracking, satellite navigation, statistics and economics.

The performance of a filter is often determined by the accuracy of the hidden state estimate it provides. The quality of estimate provided by a filter is a key factor in deciding whether a particular filter can be utilized for a particular problem or not. Oftentimes, comparison studies are conducted for various filtering techniques to find the right filter for a particular class of filtering problem.

1.1 Filtering Problem

In this thesis, the following nonlinear filtering problem is considered:

$$\frac{\mathrm{d}X_t}{\mathrm{d}t} = a(X_t) + B_t, \tag{1.1a}$$

$$Y_t = h(X_t) + W_t, \tag{1.1b}$$

where $X_t \in \mathbb{R}^d$ is the state at time t, $Y_t \in \mathbb{R}^m$ is the observation on the state, $a(\cdot)$ and $h(\cdot)$ are C^1 functions, and $\{B_t\}$, $\{W_t\}$ are mutually independent white noise processes of appropriate dimension.

The mathematical objective of the filtering problem is to approximate the posterior distribution of X_t given the history of observations, $\mathscr{Z}_t := \sigma(Z_s : s \leq t)$. The posterior denoted by p^* is defined, so that for any measurable set $A \subset \mathbb{R}^d$,

$$\int_{x \in A} p^*(x,t)\, \mathrm{d}x = \mathrm{Prob}\{X_t \in A \mid \mathscr{Z}_t\}. \tag{1.2}$$

The optimal solution for the above filtering problem is given by the Kalman filter in the case that $a(\cdot)$ and $h(\cdot)$are linear functions. If $a(\cdot)$ and $h(\cdot)$ are nonlinear functions then a nonlinear filtering algorithm is required. Earlier when the computation power is limited, the implementation of solution to this general nonlinear filtering problem by numerical approximations of such infinite dimensional stochastic evolution equations seemed impractical. Therefore, algorithms which used linear approximations to the signal-observation dynamics were studied leading to the development of the extended Kalman filter (EKF). In an extended Kalman filter, the solution to the nonlinear filtering problem is obtained by linearizing the functions $a(\cdot)$ and $h(\cdot)$ about the current state estimate and covariance and then applying the kalman algorithm to this linearized problem [**?**]. Another common approach to solve a nonlinear filtering problem is to use a particle filter. In particular we will be dealing with a new formulation of the particle filter for nonlinear filtering, the feedback particle filter (FPF) in [7, 6], which seek to utilize the concept of innovation error based feedback.

1.2 Contribution of Thesis

In this thesis, two nonlinear filtering techniques are evaluated and the performance is compared based on the criteria of state estimate accuracy for various cases.

The remainder of the thesis is organized as follows: chapter 2 provides background on the extended Kalman filter and the feedback particle filter and also describes the metrics which are be used to compare the performance. Chapter 3 introduces a scalar filtering problem, provides a list of parameters which are varied to compare the performance of the filtering methods and presents the corresponding results.

CHAPTER 2

BACKGROUND ON EKF AND FPF

This chapter provides an introduction to the algorithms used for the feedback particle filter and the extended Kalman filter. The outline of the remainder of this chapter is as follows: in section 2.1 the algorithm for the feedback particle filter is introduced, section 2.2 provides an introduction to the extended Kalman filter, and section 2.3 then describes the comparison metrics

2.1 Feedback Particle Filter

In [7, 6], the algorithm for the feedback particle filter (FPF) was introduced. FPF is a new formulation of the particle filter based on concepts from optimal control, and mean-field game theory. This is a novel algorithm for nonlinear filter and employs the principle of invoation error-base feedback structure for the control like in the case of EKF. The FPF is applicable to a general class of nonlinear filtering problems with non-Gaussian posterior distributions. The EKF, as such, is unable to handle these non-Gaussian distributions.

2.1.1 Feedback Particle Filter Algorithm

Feedback particle filter (FPF) is defined by a family of stochastic systems, which evolve under the optimal control law. Hence FPF is a system of N controlled particles. The state of the filter is $\{X_t^i : 1 \leq i \leq N\}$: The value $X_t^i \in \mathbb{R}^d$ is the state for the i^{th} particle at time t. The dynamics of the i^{th} particle have the

following gain feedback form,

$$\frac{\mathrm{d}X_t^i}{\mathrm{d}t} = a(X_t^i) + \dot{B}_t^i + \underbrace{\mathsf{K}_t\, I_t^i}_{\text{(control)}} \tag{2.1}$$

where $\{\dot{B}_t^i\}$ are mutually independent white noise processes with covariance matrix Q, and I_t^i is a modified version of the innovation process that appears in the nonlinear filter,

$$I_t^i := Y_t - \frac{1}{2}(h(X_t^i) + \hat{h}), \tag{2.2}$$

where $\hat{h} := \mathsf{E}[h(X_t^i)|\mathscr{Z}_t]$. In a numerical implementation, this is approximated to $\hat{h} \approx N^{-1}\sum_{i=1}^N h(X_t^i) =: \hat{h}^{(N)}$.

The gain function K is found as the solution to an Euler-Lagrange boundary value problem (E-L BVP): for $j = 1,2,\ldots,m$, the function ϕ_j is a solution to the second-order partial differential equation,

$$\begin{aligned} &\nabla\cdot(p(x,t)\nabla\phi_j(x,t)) = -(h_j(x) - \hat{h}_j)p(x,t), \\ &\int_{\mathbb{R}^d} \phi_j(x,t)p(x,t)\,\mathrm{d}x = 0, \end{aligned} \tag{2.3}$$

where p denotes the conditional distribution of X_t^i given $\mathscr{Z}_t$. In terms of these solutions, the gain function is given by,

$$[\mathsf{K}]_{lj}(x,t) = \sum_{s=1}^m (R^{-1})_{sj}\frac{\partial\phi_s}{\partial x_l}(x,t)\,. \tag{2.4}$$

Denoting $[D\phi] := [\nabla\phi_1,\ldots,\nabla\phi_m]$, where $\nabla\phi_j$ is a column vector for $j\in\{1,\ldots,m\}$, the gain function is succinctly expressed as a matrix product,

$$\mathsf{K} = [D\phi]R^{-1}.$$

It is shown in [7, 5] that the FPF is consistent with the nonlinear filter, given consistent initializations $p(\cdot,0) = p^*(\cdot,0)$. Consequently, if the initial conditions $\{X_0^i\}_{i=1}^N$ are drawn from the initial distribution $p^*(\cdot,0)$ of X_0, then, as $N\to\infty$, the empirical distribution of the particle system approximates the posterior distribution $p^*(\cdot,t)$ for each t.

The main computational burden of the algorithm is the computation/approximation

of the gain function at each time t. In this thesis, the gain is computed using the so-called *Galerkin approximation* [5] described in the following section.

2.1.2 Galerkin Approximation

The gain function needs to be computed at each time. For a fixed time t and $j \in \{1,\dots,m\}$, a vector-valued function $\nabla\phi_j(x,t)$ is said to be a weak solution of the BVP (2.3) if

$$\mathsf{E}\left[\nabla\phi_j \cdot \nabla\psi\right] = \mathsf{E}[(h_j - \hat{h}_j)\psi] \tag{2.5}$$

holds for all $\psi \in H^1(\mathbb{R};p)$ where $\mathsf{E}[\cdot] := \int_{\mathbb{R}^d} \cdot\, p(x,t)\,\mathrm{d}x$ and H^1 is a certain Hilbert space (see [5]). The existence-uniqueness result for the weak solution of (2.5) also appears in [5].

Since there are m uncoupled BVPs, without loss of generality, we assume scalar-valued observation in this section, with $m = 1$, so that $\mathsf{K} = \nabla\phi$. The time t is fixed. The explicit dependence on time is suppressed for notational ease (That is, $p(x,t)$ is denoted as $p(x)$, $\phi(x,t)$ as $\phi(x)$ etc.).

Using (2.5), the gain function $\mathsf{K} = \nabla\phi$ is a weak solution if

$$\mathsf{E}[\mathsf{K}\cdot\nabla\psi] = \mathsf{E}[(h-\hat{h})\psi], \quad \forall\ \psi \in H^1(\mathbb{R}^d;p). \tag{2.6}$$

The gain function is approximated as,

$$\mathsf{K} = \sum_{l=1}^{L} \kappa_l \chi_l(x),$$

where $\{\chi_l(x)\}_{l=1}^L$ are *basis functions*. For each $l = 1,\dots,L$, $\chi_l(x)$ is a gradient function; That is, $\chi_l(x) = \nabla\zeta_l(x)$ for some function $\zeta_l(x) \in H^1_0(\mathbb{R}^d;p)$.

The *test functions* are denoted as $\{\psi_k(x)\}_{k=1}^L$ and $S := \mathrm{span}\{\psi_1(x),\psi_2(x),\dots,\psi_L(x)\} \subset H^1(\mathbb{R}^d;p)$.

The finite-dimensional approximation of the BVP (2.6) is to choose constants $\{\kappa_l\}_{l=1}^L$ such that

$$\sum_{l=1}^{L} \kappa_l \mathsf{E}[\chi_l\cdot\nabla\psi] = \mathsf{E}[(h-\hat{h})\psi], \quad \forall\ \psi \in S. \tag{2.7}$$

Denoting $[A]_{kl} = \mathsf{E}[\chi_l \cdot \nabla \psi_k]$, $b_k = \mathsf{E}[(h - \hat{h})\psi_k]$, $\kappa = (\kappa_1, \kappa_2, \ldots, \kappa_L)^T$, the finite-dimensional approximation (2.7) is expressed as a linear matrix equation:

$$A\kappa = b.$$

The matrix A and vector b are easily approximated by using only the particles:

$$[A]_{kl} = \mathsf{E}[\chi_l \cdot \nabla \psi_k] \approx \frac{1}{N}\sum_{i=1}^{N} \chi_l(X_t^i) \cdot \nabla \psi_k(X_t^i), \tag{2.8}$$

$$b_k = \mathsf{E}[(h - \hat{h})\psi_k] \approx \frac{1}{N}\sum_{i=1}^{N} (h(X_t^i) - \hat{h})\psi_k(X_t^i), \tag{2.9}$$

where recall $\hat{h} \approx \frac{1}{N}\sum_{i=1}^{N} h(X_t^i)$.

2.1.3 Constant Gain Approximation

Suppose $\chi_l = e_l$, the canonical coordinate vector with value 1 for the l^{th} coordiate and zero otherwise. The test functions are the coordinate functions $\psi_k(x) = x_k$ for $k = 1, 2, \ldots, d$. Denoting $\psi(x) = (\psi_1, \psi_2, \ldots, \psi_d)^T = x$,

$$\begin{aligned} \kappa = \mathsf{E}[\mathsf{K}] = \mathsf{E}[(h - \hat{h})\psi] &= \int (h(x) - \hat{h})\psi(x)p(x)\,\mathrm{d}x \\ &\approx \frac{1}{N}\sum_{i=1}^{N} (h(X_t^i) - \hat{h})X_t^i. \end{aligned} \tag{2.10}$$

This formula yields the *constant-gain approximation* of the gain function.

It is interesting to note that for the linear-Gaussian case, this constant approximation for the gain function yields the same result as the Kalman gain. Also In [3, 4, 2], it has been showed that the FPF-based implementations retain the innovation error-based feedback structure even for the nonlinear problem.

2.2 Extended Kalman Filter

Extended Kalman filter (EKF) is an extension of the Kalman filter algorithm, that linearizes about the current state estimate and covariance. The algorithm is

used to obtain an approximate solution to the nonlinear filtering problem. The EKF approximates the posterior distribution by a Gaussian distribution, parameterized by its mean $\hat{X}_t$ and the covariance matrix P_t.

To perform the update step, the EKF uses linearizations of the signal model $a(\cdot)$ and the observation model $h(\cdot)$, evaluated at the mean $\hat{X}_t$. The respective Jacobian matrices are denoted by $A := \frac{\partial a}{\partial x}(\hat{X}_t)$ and $H := \frac{\partial h}{\partial x}(\hat{X}_t)$.

The EKF algorithm is given by,

$$\frac{\mathrm{d}\hat{X}_t}{\mathrm{d}t} = a(\hat{X}_t) + \mathsf{K}_t \left(Y_t - h(\hat{X}_t)\right), \tag{2.11}$$

$$\frac{\mathrm{d}P_t}{\mathrm{d}t} = AP_t + P_t A^T + Q - \mathsf{K}_t H P_t. \tag{2.12}$$

where the Kalman gain

$$\mathsf{K}_t = P_t H^T R^{-1}. \tag{2.13}$$

Under the assumptions that the signal and the observation models are linear and the posterior distribution is Gaussian, the Kalman filter is the optimal solution. For non-Gaussian and strongly nonlinear problems, the EKF algorithm is known to perform poorly, and can suffer from divergence issues; cf., [1].

2.3 Comparison metrics

The performance of the filters is evaluated based on the following two metrics:

1. Mean squared error in X_t

$$\text{error in } X_t = \frac{\int_0^t (\hat{X}_t - X_t)^2 dt}{\int_0^t X_t^2 dt} \tag{2.14}$$

2. Mean squared error in h_t

$$\text{error in } h_t = \frac{\int_0^t (\hat{h}_t - h_t)^2 dt}{\int_0^t h_t^2 dt} \tag{2.15}$$

CHAPTER 3

COMPARISON STUDIES

In this chapter we will consider the simplest possible filtering filtering problem which has linear signal dynamics and nonlinear observation dynamics. Different parameters of the signal and observation model will be varied and performance of the two filtering techniques, FPF and EKF is compared based on the two comparison metrics (2.14), (2.15) defined in the previous section. The outline of this chapter is as follows: Section 3.1 introduces the state dynamics and observation dynamics of the filtering problem. Section 3.2 describes different instances of the EKF and FPF which will be compared. Section 3.3 introduces the various parameters of the signal and observation model which will be varied to compare the performance of the filters and their corresponding results

3.1 Filtering problem

A. Signal model

The state of the signal process X_t evolves according to,

$$\frac{\mathrm{d}X_t}{\mathrm{d}t} = a + B_t \tag{3.1}$$

$\{B_t\}$ is a white noise process characterized by covariance σ_b.

The signal model is initialized according to the parameter values defined in Table 3.1

Table 3.1: Signal model initialization

Parameter	Initial value (X_0)	a	σ_b
Value	0	2π	0.1

B. Observation model

The observation model is given by

$$Y_t = h(X_t) + W_t, \tag{3.2}$$

where, $h(x) = c_0 + c_1\cos(x) + s_1\sin(x) + c_2\cos(2x) + s_2\sin(2x)$

$\{W_t\}$ is a white noise process characterized by covariance σ_w.

The signal model is initialized according to the parameter values defined in Table 3.2

Table 3.2: Observation model initialization

Parameter	c_0	c_1	s_1	c_2	s_2	σ_w
Value	1	1	1	1	1	0.01

3.2 Initialization of Filters

The performance of the following instances of extended Kalman filter and feedback particle filter is compared:

i. extended Kalman filter with low process noise covariance ($Q = 0.1^2$)

ii. extended Kalman filter with high process noise covariance ($Q = 1$)

iii. feedback particle filter with 50 particles

iv. feedback particle filter with 500 particles

The above four filters are initialized according to the parameter values defined in Table 3.3

Table 3.3: Filter initialization

Parameter	EKF($Q = 0.1^2$)	EKF($Q = 1$)	FPF(50 particles)	FPF(500 particles)
Initial condition	$X_0 = 0$	$X_0 = 0$	$X_0^i \in uniform(0, 2\pi)$	$X_0^i \in uniform(0, 2\pi)$
Model parameter	$a = 2\pi$	$a = 2\pi$	$a^i \in uniform(1.8\pi, 2.2\pi)$	$a^i \in uniform(1.8\pi, 2.2\pi)$
Process noise	$Q = 0.1^2$	$Q = 1$	$\sigma_b^2 = 0.0$	$\sigma_b^2 = 0.0$
Observation noise	$R = 0.1^2$	$R = 0.1^2$	$\sigma_w^2 = 0.1^2$	$\sigma_w^2 = 0.1^2$
	$P_0 = \pi^2/3$	$P_0 = \pi^2/3$	N = 50 particles	N = 500 particles

3.3 Comparison study

The performance of the four filters is compared with respect to the following parameters:

i. initial condition of the signal model

ii. model parameter a of the signal model

iii. process noise σ_b

iv. observation noise σ_w

v. unknown observation model dynamics

3.3.1 Initial condition of the signal model

The initial condition of the signal model is varied and the accuracy of the state estimate obtained from the filters is compared using the metrics defined in (2.14), (2.15). The rest of the parameters of the signal model and observation model are left unchanged. The filters are intialized to the parameter values defined in Table 3.3.

The initial condition of the signal model is varied from 0 to 2π in steps of 0.1π and the corresponding error values are calculated for each of the four filters. The following figures Fig. 3.1, Fig. 3.2 show the errors in $\hat{X}_t$ and $\hat{h}_t$ of the filters for the corresponding initial condition of the signal model.

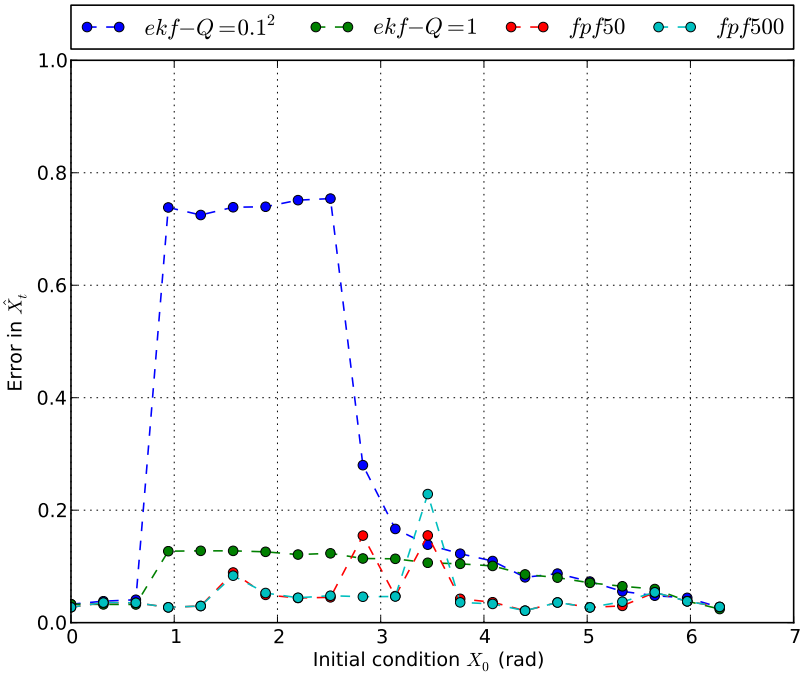

Figure 3.1: X-error vs IC

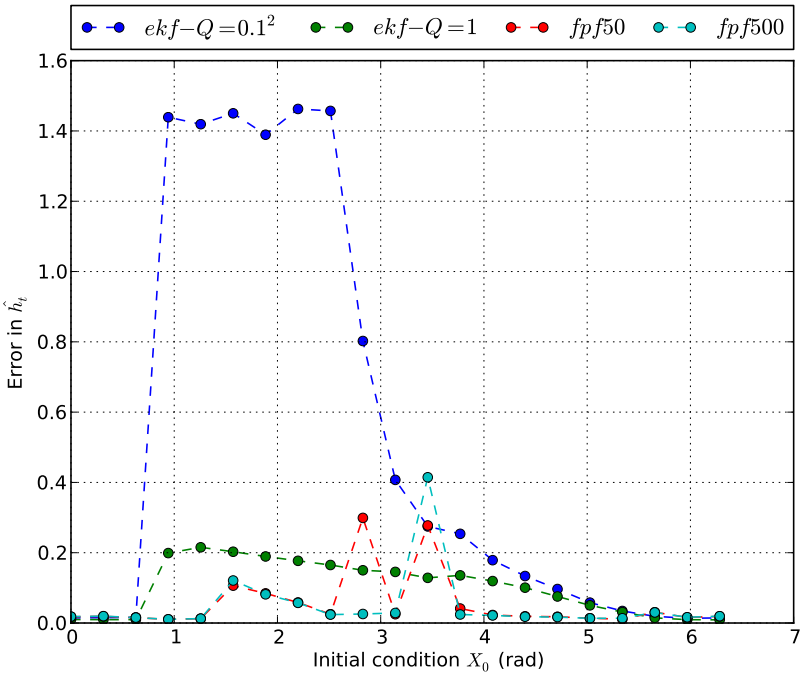

Figure 3.2: h-error vs IC

It can be observed from the plots that there are two values of the initial condi-

tions, one around $pi/2$ and the other around pi, where sudden increase in the error values of FPF's can be seen. This might be because the particles do not converge around these two values.

To observe the effects of observation noise of the filters on the performance of the filters, the above process is repeated for two other values of observation noise i.e., σ_w of the filters

i. $R = \sigma_w^2 = 0.05^2$ and

ii. $R = \sigma_w^2 = 0.5^2$

i. $R = \sigma_w^2 = 0.05^2$

The filters are intialized to the parameter values defined in Table 3.4. Except for the observation noise (R = σ_w^2) value, all the other parameters are intialized to exactly the same values defined in Table 3.3

Table 3.4: Filter initialization

Parameter	EKF($Q = 0.1^2$)	EKF($Q = 1$)	FPF(50 particles)	FPF(500 particles)
Initial condition	$X_0 = 0$	$X_0 = 0$	$X_0^i \in uniform(0, 2\pi)$	$X_0^i \in uniform(0, 2\pi)$
Model parameter	$a = 2\pi$	$a = 2\pi$	$a^i \in uniform(1.8\pi, 2.2\pi)$	$a^i \in uniform(1.8\pi, 2.2\pi)$
Process noise	$Q = 0.1^2$	$Q = 1$	$\sigma_b^2 = 0.0$	$\sigma_b^2 = 0.0$
Observation noise	$R = 0.05^2$	$R = 0.05^2$	$\sigma_w^2 = 0.05^2$	$\sigma_w^2 = 0.05^2$
	$P_0 = \pi^2/3$	$P_0 = \pi^2/3$	N = 50 particles	N = 500 particles

The initial condition of the signal model is varied from 0 to 2π in steps of 0.1π and the corresponding error values are calculated for each of the four filters. The following figures Fig. 3.3, Fig. 3.4 show the errors in $\hat{X}_t$ and $\hat{h}_t$ of the filters for the corresponding initial condition of the signal model.

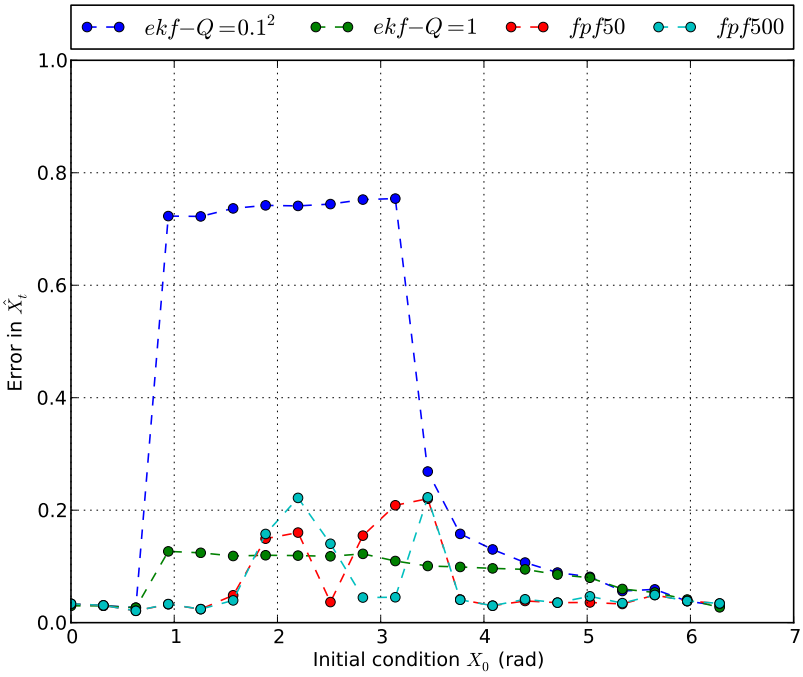

Figure 3.3: X-error vs IC

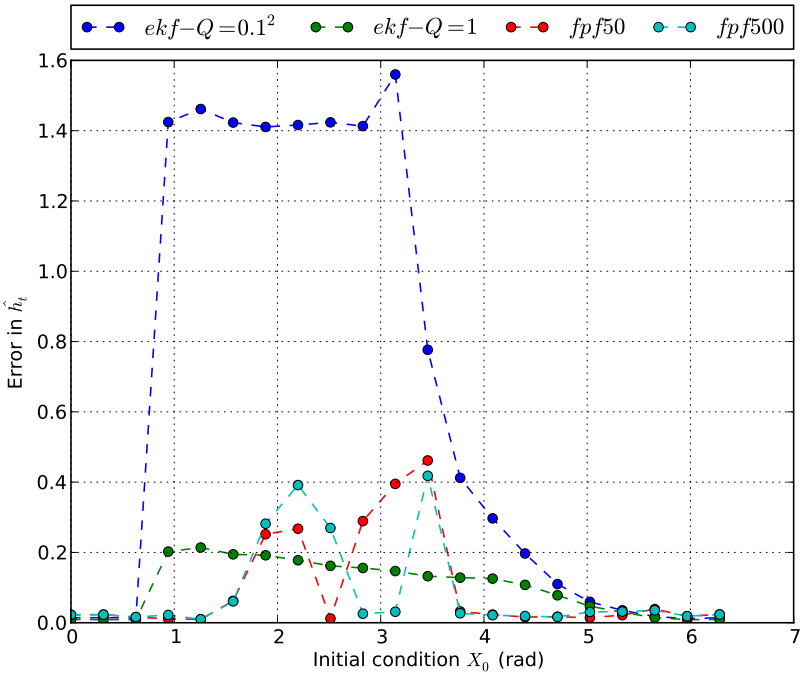

Figure 3.4: h-error vs IC

ii. $R = \sigma_w^2 = 0.5^2$

The filters are intialized to the parameter values defined in Table 3.5. Except for the observation noise (R = σ_w^2) value, all the other parameters are intialized to exactly the same values defined in Table 3.3

Table 3.5: Filter initialization

Parameter	EKF($Q = 0.1^2$)	EKF($Q = 1$)	FPF(50 particles)	FPF(500 particles)
Initial condition	$X_0 = 0$	$X_0 = 0$	$X_0^i \in uniform(0, 2\pi)$	$X_0^i \in uniform(0, 2\pi)$
Model parameter	$a = 2\pi$	$a = 2\pi$	$a^i \in uniform(1.8\pi, 2.2\pi)$	$a^i \in uniform(1.8\pi, 2.2\pi)$
Process noise	$Q = 0.1^2$	$Q = 1$	$\sigma_b^2 = 0.0$	$\sigma_b^2 = 0.0$
Observation noise	$R = 0.5^2$	$R = 0.5^2$	$\sigma_w^2 = 0.5^2$	$\sigma_w^2 = 0.5^2$
	$P_0 = \pi^2/3$	$P_0 = \pi^2/3$	N = 50 particles	N = 500 particles

The initial condition of the signal model is varied from 0 to 2π in steps of 0.1π and the corresponding error values are calculated for each of the four filters. The following figures Fig. 3.5, Fig. 3.6 show the errors in $\hat{X}_t$ and $\hat{h}_t$ of the filters for the corresponding initial condition of the signal model.

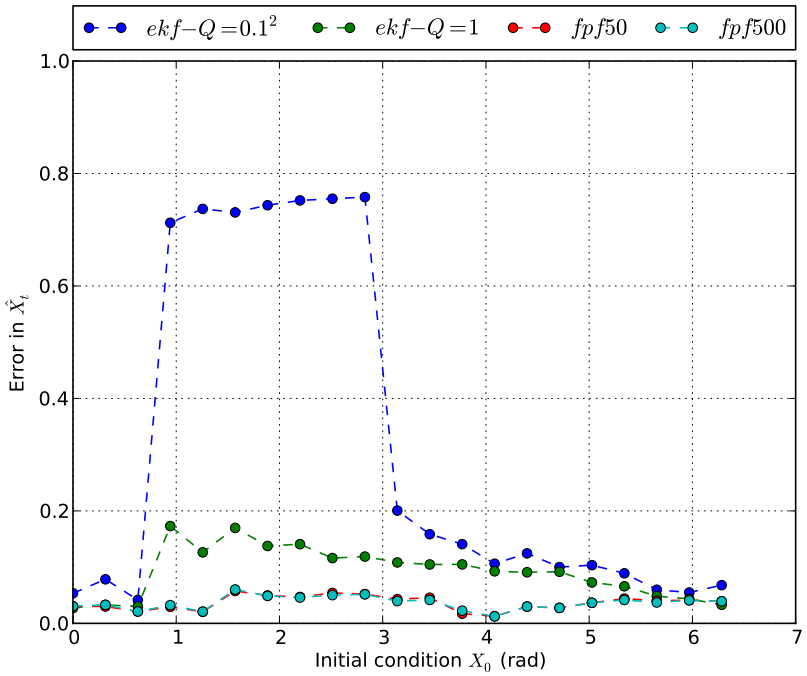

Figure 3.5: X-error vs IC

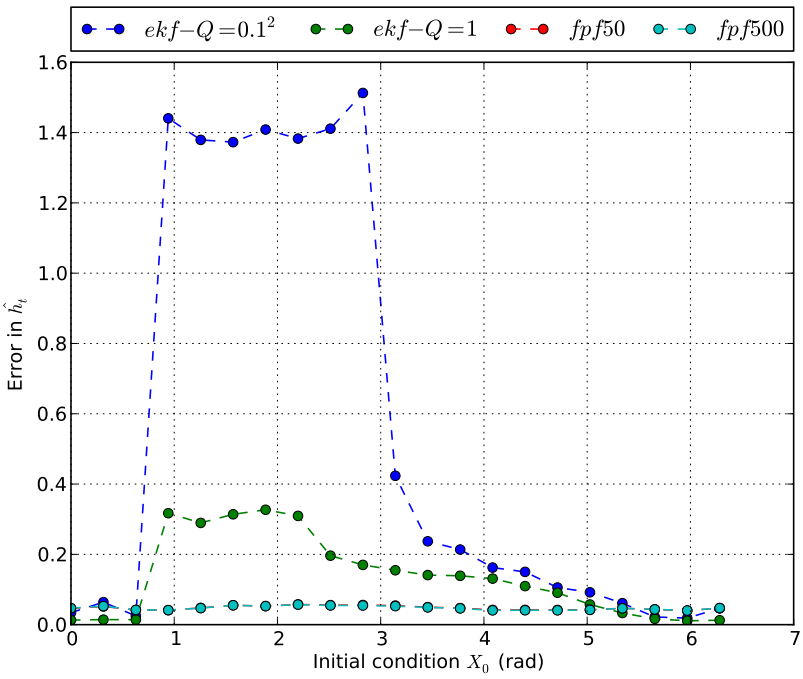

Figure 3.6: h-error vs IC

Comparing the three cases against each other, it can be observed that the performance of the EKF filters with respect to the changes in initial conditions, is fairly invariant to the changes in the observation noise covariance of the filters. The performance of the FPF's on the other hand, although not by much, seems to increase with the increase in the observation noise covariance of the filters. It can also be observed that the sudden increase in error around $\pi/2$ and π go away as the observation noise covariance of the filters is increased.

From the above plots for the case with $\sigma_w^2 = 0.5^2$, the following observations can be made:

i. The errors in both $\hat{X}_t$ and $\hat{h}_t$ are very low for the two instances of FPF, one with 50 particles and the other with 500 particles. This indicates that the state estimate obtained from these two filters is very close to the actual state of the signal model. This suggests that the FPF filtering technique is fairly robust to the changes in initial conditions of the signal model and the performance is not dependent on the accuracy of the initial guess of the actual initial condition of the signal model.

ii. In the case of EKF with low process noise covariance, i.e., $Q = 0.1^2$, when

the initial condition of the signal model is close to that of the initial guess of the filter i.e., 0, the filter has done well which can be seen from low errors in $\hat{X}_t$ and $\hat{h}_t$. But as the initial value of the signal model moves away from 0, the errors in both $\hat{X}_t$ and $\hat{h}_t$ shoot up rapidly suggesting that the state estimate obtained from the filter is not a very accurate guess of the actual state of the signal model. But then again as the initial condition of the signal model moves closer to 2π, the errors. This instance of the EKF filter performs very poorly when we don't have a good guess of the actual initial value of the signal model hence requires a reasonably accurate guess of the actual initial condition of the signal model to perform well.

iii. In the case of EKF with high process noise covariance, i.e., $Q = 1$, a significant improvement in the performance from the other instance of EKF can be seen. The errors in both $\hat{X}_t$ and $\hat{h}_t$ are lower than those of EKF with $Q = 0.1^2$ but higher than the two instances of FPF.

iv. It can also be seen that that when the initial guess of the filter is close to actual initial value of the signal model, performance of all the four filters is nearly the same.

v. When the initial guess is far from the actual initial value of the signal model, the FPF's outperform both the instances of EKF. From the plots it can be concluded that the performance of
FPF with 500 particles $\approx$ FPF with 50 particles $>$ EKF with $Q = 1 >$ EKF with $Q = 0.1^2$

iii. Low initial covariance ($P_0 = 0.1$) for EKF

In this section, the effects of starting the EKF's with a low initial covariance value on the performance of the filters will be observed. The filters are intialized to the parameter values defined in Table 3.6. Except for the initial covariance (P_0) value of the two EKF's, all the other parameters are intialized to exactly the same values defined in Table 3.5

Table 3.6: Filter initialization

Parameter	EKF($Q = 0.1^2$)	EKF($Q = 1$)	FPF(50 particles)	FPF(500 particles)
Initial condition	$X_0 = 0$	$X_0 = 0$	$X_0^i \in uniform(0, 2\pi)$	$X_0^i \in uniform(0, 2\pi)$
Model parameter	$a = 2\pi$	$a = 2\pi$	$a^i \in uniform(1.8\pi, 2.2\pi)$	$a^i \in uniform(1.8\pi, 2.2\pi)$
Process noise	$Q = 0.1^2$	$Q = 1$	$\sigma_b^2 = 0.0$	$\sigma_b^2 = 0.0$
Observation noise	$R = 0.5^2$	$R = 0.5^2$	$\sigma_w^2 = 0.5^2$	$\sigma_w^2 = 0.5^2$
	$P_0 = 0.1$	$P_0 = 0.1$	N = 50 particles	N = 500 particles

The initial condition of the signal model is varied from 0 to 2π in steps of 0.1π and the corresponding error values are calculated for each of the four filters. The following figures Fig. 3.7, Fig. 3.8 show the errors in $\hat{X}_t$ and $\hat{h}_t$ of the filters for the corresponding initial condition of the signal model.

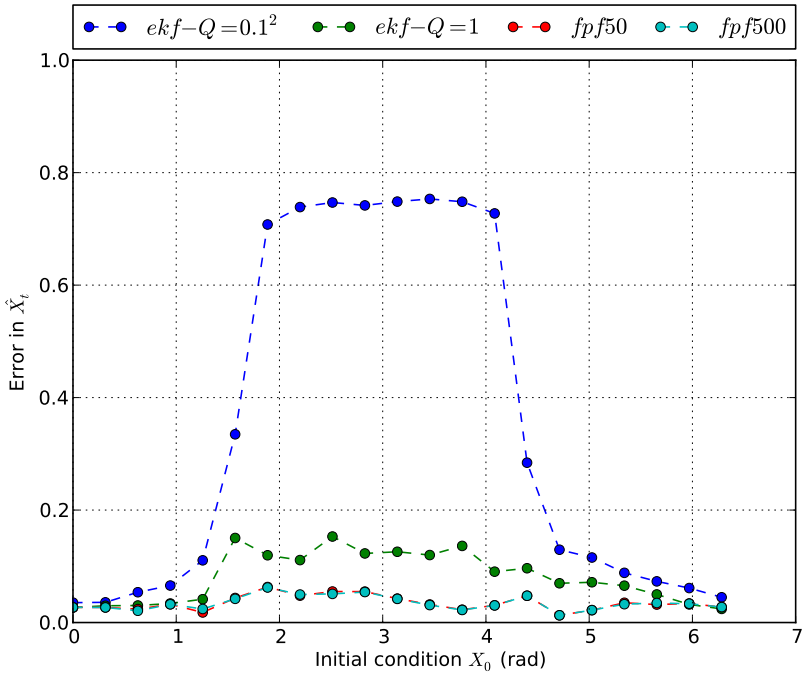

Figure 3.7: X-error vs IC

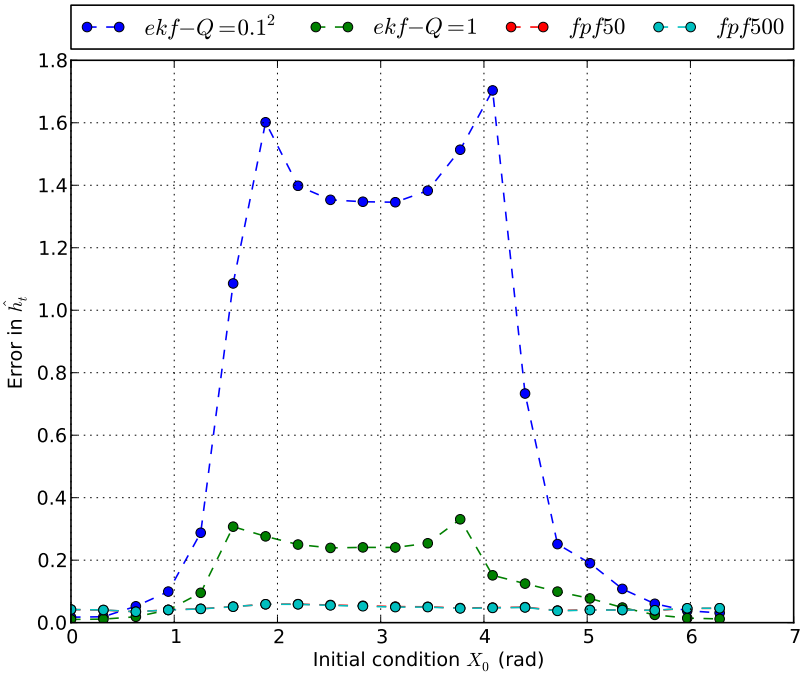

Figure 3.8: h-error vs IC

With a lower value of the initial covariance P_0, the instance of EKF with $Q = 0.1^2$ seems to perform well for a larger spread of initial values around zero. It can be observed that in the previous case with a larger covariance, the error in $\hat{X}_t$ and $\hat{h}_t$ shoot up drastically at around 0.3π while now this seems to happen at around 0.6π. On the otherhand, the performance of the EKF with $Q = 1$ remained fairly invariant to the change in intial covariance P_0.

3.3.2 Model parameter a of the signal model

In this section the model parameter a of the signal model is varied and the accuracy of the state estimate obtained from the filters is compared using the metrics defined in (2.14), (2.15). The rest of the parameters of the signal model and observation model are set to the values defined in Tables 3.1, 3.2. The filters are initalized to the parameter values defined in Table 3.7

Table 3.7: Filter initialization

Parameter	EKF($Q = 0.1^2$)	EKF($Q = 1$)	FPF(50 particles)	FPF(500 particles)
Initial condition	$X_0 = 0$	$X_0 = 0$	$X_0^i \in uniform(0, 2\pi)$	$X_0^i \in uniform(0, 2\pi)$
Model parameter	$a = 2\pi$	$a = 2\pi$	$a^i \in uniform(1.8\pi, 2.2\pi)$	$a^i \in uniform(1.8\pi, 2.2\pi)$
Process noise	$Q = 0.1^2$	$Q = 1$	$\sigma_b^2 = 0.0$	$\sigma_b^2 = 0.0$
Observation noise	$R = 0.1^2$	$R = 0.1^2$	$\sigma_w^2 = 0.1^2$	$\sigma_w^2 = 0.1^2$
	$P_0 = \pi^2/3$	$P_0 = \pi^2/3$	N = 50 particles	N = 500 particles

The model parameter a of the signal model is varied from $0.5 * 2\pi$ to $1.5 * 2\pi$ in steps of $0.05 * 2\pi$, which corresposnds to increasing the frequency from 0.5 to 1.5 in steps of 0.05. The corresponding error values are calculated for each of the four filters. The following figures Fig. 3.9, Fig. 3.10 show the errors in $\hat{X}_t$ and $\hat{h}_t$ of the filters for the corresponding frequency of the signal model.

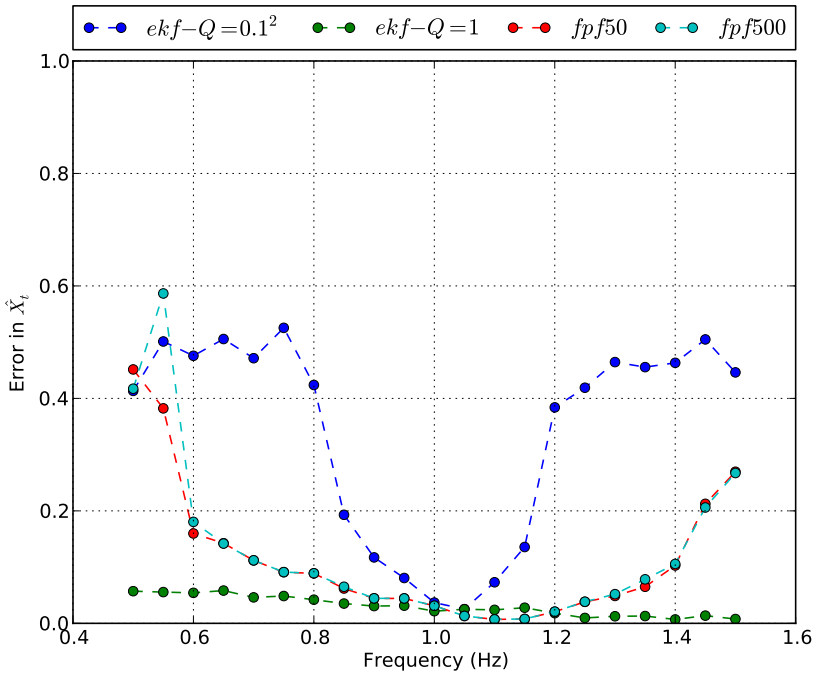

Figure 3.9: X-error vs frequency

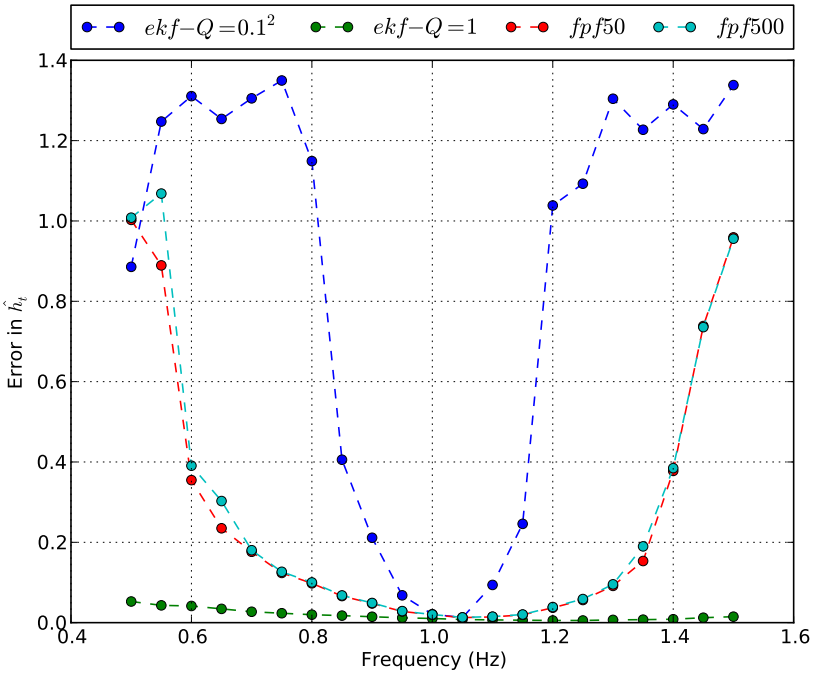

Figure 3.10: h-error vs frequency

To observe the effects of observation noise of the filters on the performance of the filters, the above process is repeated for two other values of observation noise i.e., σ_w of the filters

i. $R = \sigma_w^2 = 0.05^2$ and

ii. $R = \sigma_w^2 = 0.5^2$

i. $R = \sigma_w^2 = 0.05^2$

The filters are intialized to the parameter values defined in Table 3.8. Except for the observation noise (R = σ_w^2) value, all the other parameters are intialized to exactly the same values defined in Table 3.7

Table 3.8: Filter initialization

Parameter	EKF($Q = 0.1^2$)	EKF($Q = 1$)	FPF(50 particles)	FPF(500 particles)
Initial condition	$X_0 = 0$	$X_0 = 0$	$X_0^i \in uniform(0, 2\pi)$	$X_0^i \in uniform(0, 2\pi)$
Model parameter	$a = 2\pi$	$a = 2\pi$	$a^i \in uniform(1.8\pi, 2.2\pi)$	$a^i \in uniform(1.8\pi, 2.2\pi)$
Process noise	$Q = 0.1^2$	$Q = 1$	$\sigma_b^2 = 0.0$	$\sigma_b^2 = 0.0$
Observation noise	$R = 0.05^2$	$R = 0.05^2$	$\sigma_w^2 = 0.05^2$	$\sigma_w^2 = 0.05^2$
	$P_0 = \pi^2/3$	$P_0 = \pi^2/3$	N = 50 particles	N = 500 particles

The model parameter a of the signal model is varied from $0.5 * 2\pi$ to $1.5 * 2\pi$ in steps of $0.05 * 2\pi$, which corresposnds to increasing the frequency from 0.5 to 1.5 in steps of 0.05. The corresponding error values are calculated for each of the four filters. The following figures Fig. 3.11, Fig. 3.12 show the errors in $\hat{X}_t$ and $\hat{h}_t$ of the filters for the corresponding frequency of the signal model.

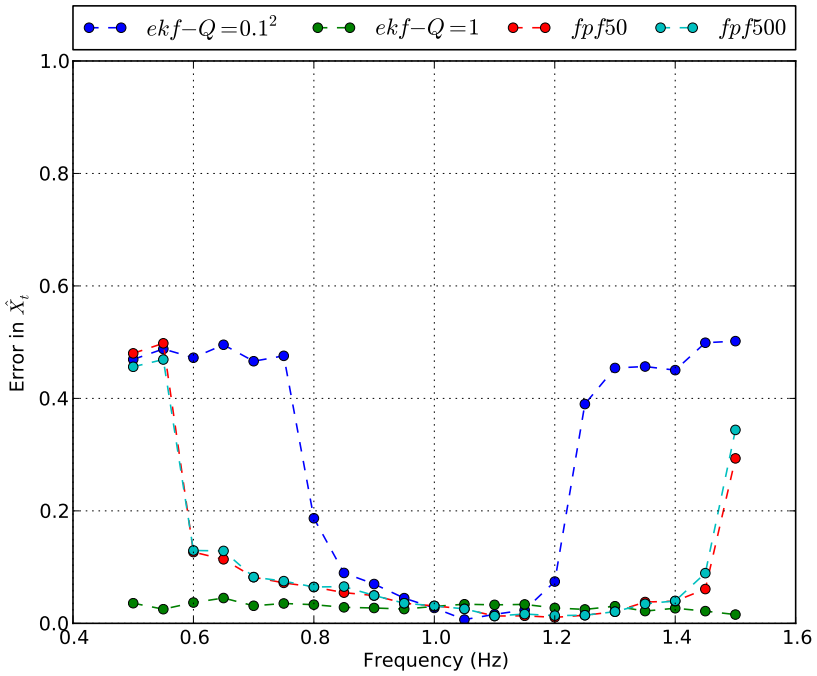

Figure 3.11: X-error vs frequency

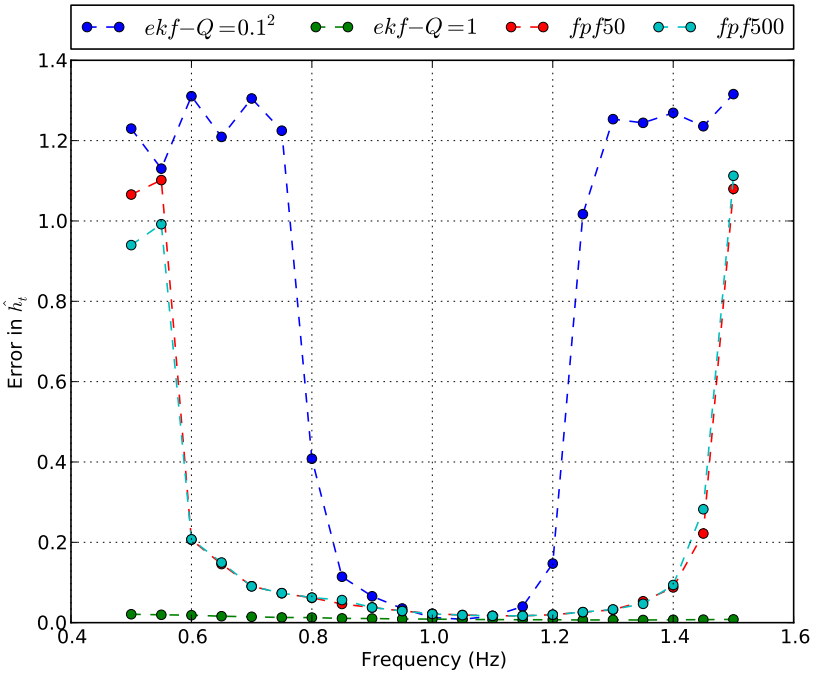

Figure 3.12: h-error vs frequency

ii. $R = \sigma_w^2 = 0.5^2$

The filters are intialized to the parameter values defined in Table 3.9. Except for the observation noise (R = σ_w^2) value, all the other parameters are intialized to exactly the same values defined in Table 3.7

Table 3.9: Filter initialization

Parameter	EKF($Q = 0.1^2$)	EKF($Q = 1$)	FPF(50 particles)	FPF(500 particles)
Initial condition	$X_0 = 0$	$X_0 = 0$	$X_0^i \in uniform(0, 2\pi)$	$X_0^i \in uniform(0, 2\pi)$
Model parameter	$a = 2\pi$	$a = 2\pi$	$a^i \in uniform(1.8\pi, 2.2\pi)$	$a^i \in uniform(1.8\pi, 2.2\pi)$
Process noise	$Q = 0.1^2$	$Q = 1$	$\sigma_b^2 = 0.0$	$\sigma_b^2 = 0.0$
Observation noise	$R = 0.5^2$	$R = 0.5^2$	$\sigma_w^2 = 0.5^2$	$\sigma_w^2 = 0.5^2$
	$P_0 = \pi^2/3$	$P_0 = \pi^2/3$	N = 50 particles	N = 500 particles

Again, the model parameter a of the signal model is varied from $0.5 * 2\pi$ to $1.5 * 2\pi$ in steps of $0.05 * 2\pi$, which corresposnds to increasing the frequency from 0.5 to 1.5 in steps of 0.05. The corresponding error values are calculated for each of the four filters. The following figures Fig. 3.13, Fig. 3.14 show the errors in $\hat{X}_t$ and $\hat{h}_t$ of the filters for the corresponding frequency of the signal model.

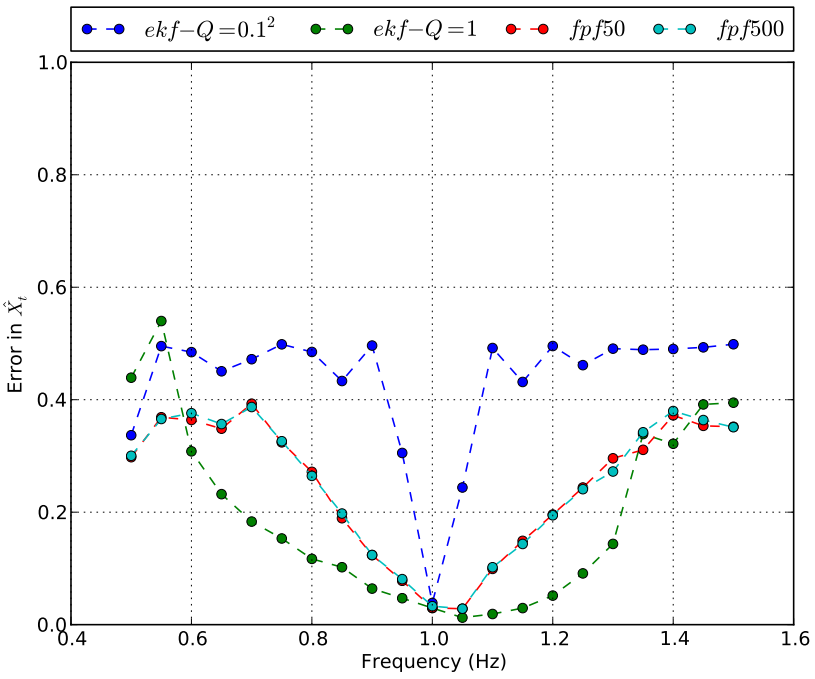

Figure 3.13: X-error vs frequency

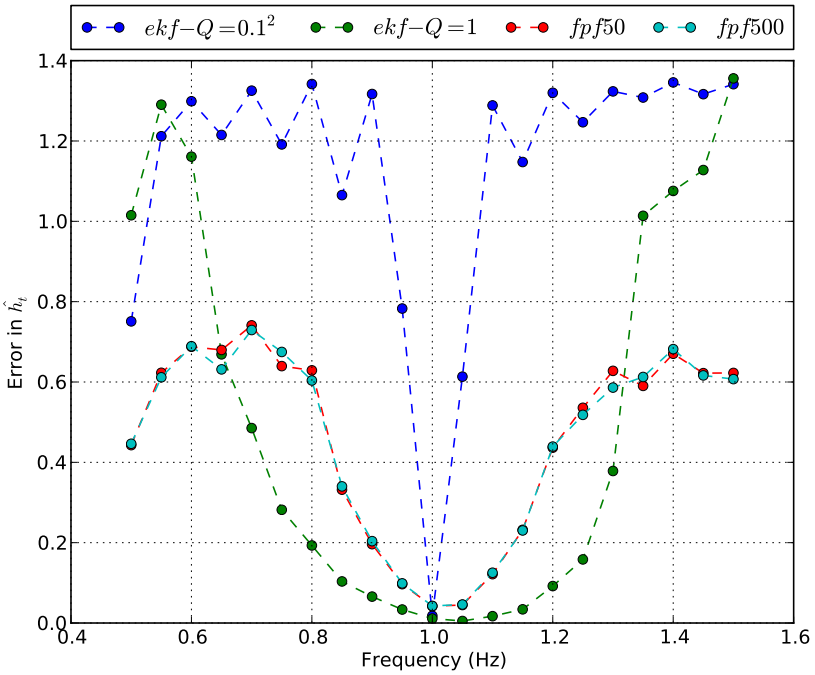

Figure 3.14: h-error vs frequency

//

Comparing the three cases against each other, it can be observed that the error curves for all the four filters are more flatter in the case with lower observation noise which indicates lower errors and better state estimates from the filters. Hence the performance of all the four filters with respect to changes in model parameter a of the signal model increased by decreasing the observation noise covariance of the filters.

The case with filter observation noise convariance of $\sigma_w^2 = 0.05^2$ is considered to make the following observations:

i. The errors in both $\hat{X}_t$ and $\hat{h}_t$ are low for both the instances of FPF, for most of the values of model parameter a of the signal model. This indicates that the state estimate from these two filters is close to the actual state of the signal. This suggests that when started with a value of model parameter a different from that of the signal model, the FPF's are able to cope with the difference. We can say that both the FPF's are fairly robust to the changes in model parameter a of the signal model and the performance is not dependent on the accuracy of the value of a with which the particles are initialized.

ii. In the case of EKF with low process noise covariance, i.e., $Q = 0.1^2$, when the value of model parameter a of the signal model is close to the value with which the filter is initialized, the filter perfomed really well which can be concluded from the low errors in $\hat{X}_t$ and $\hat{h}_t$. But as the value of a of the signal model moves away from the model parameter value of the filter, the errors in both $\hat{X}_t$ and $\hat{h}_t$ shoot up rapidly indicating that this instance of EKF is not able to cope up with large changes in model parameter a of the signal. Hence this instance of EKF is not robust to changes in model parameter of the signal and the performance of the filter is dependent on the accuracy of the value of a with which the filter is initialized. The closer the model parameter a of the filter is to that of the signal model, the better the performance of the filter is.

iii. In the case of EKF with high process noise covariance, i.e., $Q = 1$, it can be observed that the errors in both $\hat{X}_t$ and $\hat{h}_t$ are very low for all the values of model parameter a of the signal model. Hence this instance of EKF is very robust to changes in model parameter of the signal model and the performance of the filter is independent on the accuracy of the model parameter value with which the filter is initialized.

iv. When the model parameter a of the filter is close to that of the signal model, performance of all the four filters is comparable

v. When the model parameter a of the filter is not close to the actual model a of the signal model, the EKF with $Q = 1$ outperforms both the instances of FPF and EKF with $Q = 0.1^2$. From the plots it can be concluded that the performance of
EKF with $Q = 1 >$ FPF with 500 particles $\approx$ FPF with 50 particles $>$ EKF with $Q = 0.1^2$

iii. Variation in spread of particle model parameter vallues for FPF's

In this section, the effects of changing the initial spread of particle model parameter values on the performance of the FPF's will be observed. The filters are intialized to the parameter values defined in Table 3.10. Only the model parameter values of the two instances of FPF are varied and rest of the parameters are left unchanged.

Table 3.10: Filter initialization

Parameter	EKF($Q = 0.1^2$)	EKF($Q = 1$)	FPF(50 particles)	FPF(500 particles)
Initial condition	$X_0 = 0$	$X_0 = 0$	$X_0^i \in uniform(0, 2\pi)$	$X_0^i \in uniform(0, 2\pi)$
Model parameter	$a = 2\pi$	$a = 2\pi$	$a^i \in uniform(1.8\pi, 2.2\pi)$	$a^i \in uniform(1.8\pi, 2.2\pi)$
Process noise	$Q = 0.1^2$	$Q = 1$	$\sigma_b^2 = 0.0$	$\sigma_b^2 = 0.0$
Observation noise	$R = 0.05^2$	$R = 0.05^2$	$\sigma_w^2 = 0.05^2$	$\sigma_w^2 = 0.05^2$
	$P_0 = \pi^2/3$	$P_0 = \pi^2/3$	N = 50 particles	N = 500 particles

The model parameter a of the signal model is varied from $0.5 * 2\pi$ to $1.5 * 2\pi$ in steps of $0.05 * 2\pi$ and the corresponding error values are calculated for each of the four filters for the following cases:

i. $a^i \in uniform(1.6\pi, 2.4\pi)$
The following figure Fig. 3.15 shows the error in $\hat{X}_t$.

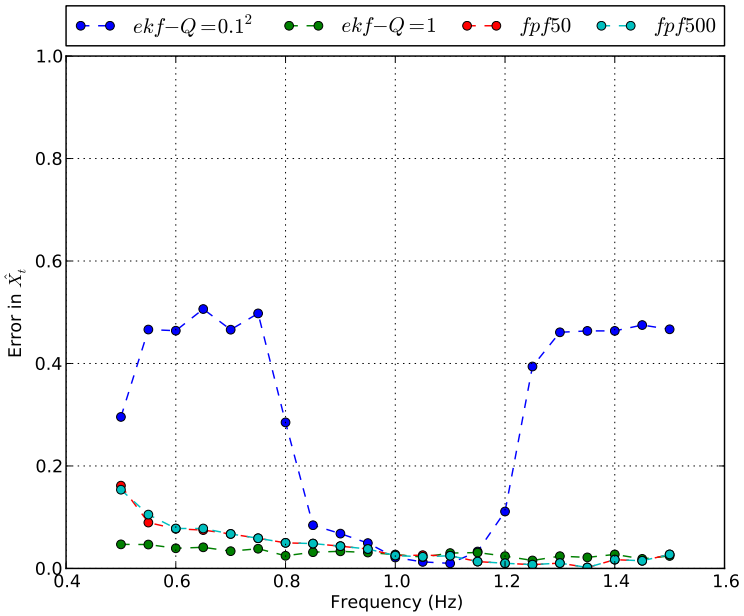

Figure 3.15: X-error vs frequency

ii. $a^i \in uniform(1.4\pi, 2.6\pi)$

The following figure Fig. 3.16 shows the error in $\hat{X}_t$.

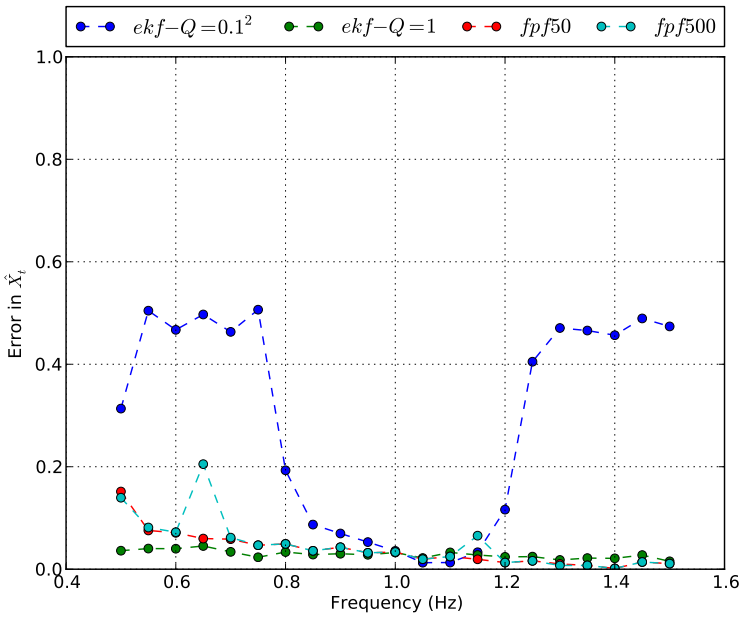

Figure 3.16: X-error vs frequency

iii. $a^i \in uniform(1.2\pi, 2.8\pi)$

The following figure Fig. 3.17 shows the error in $\hat{X}_t$.

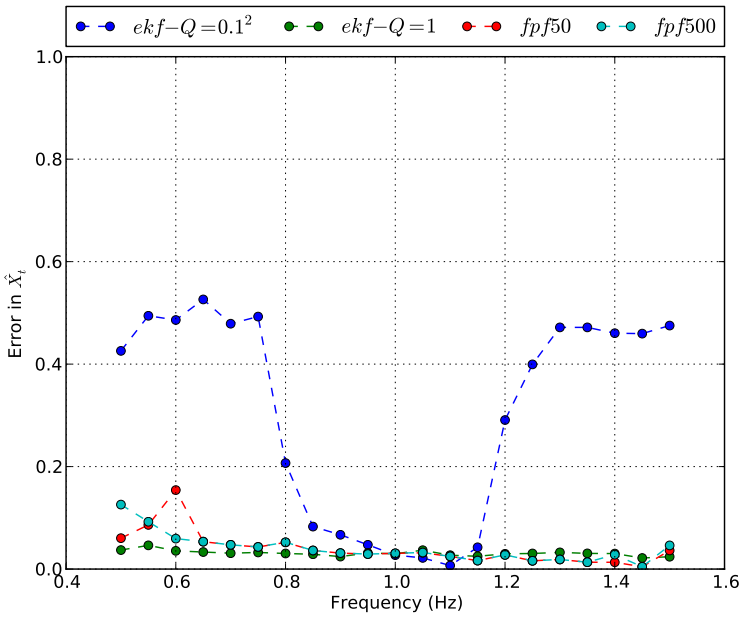

Figure 3.17: X-error vs frequency

iv. $a^i \in uniform(1.0\pi, 3.0\pi)$

The following figure Fig. 3.18 shows the error in $\hat{X}_t$.

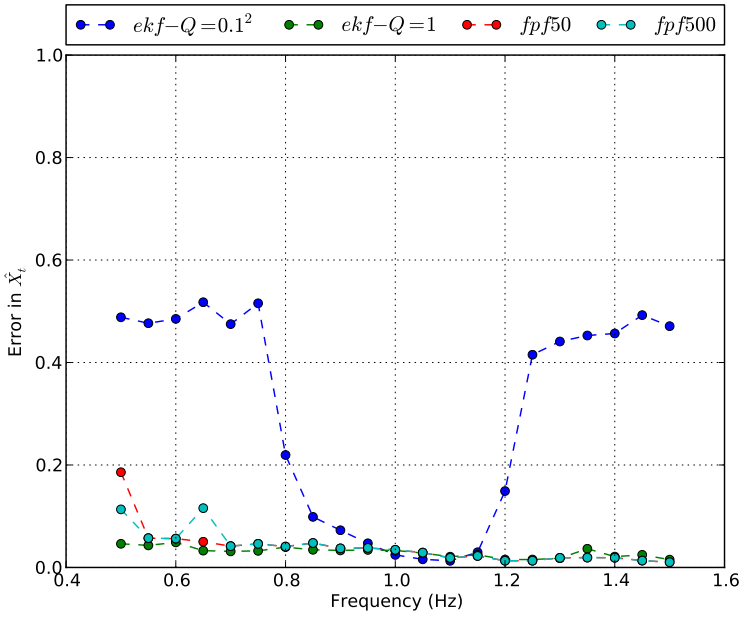

Figure 3.18: X-error vs frequency

From the above plots it can be concluded that the wider the spread of the model parameter value of the particles, the better it performs when the actual value of a of the signal model deviates from the approximate guess around which the particle model parameter values are initialized.

3.3.3 Process noise σ_b

In this section the process noise covariance σ_b of the signal model is varied and the accuracy of the state estimate obtained from the filters is compared using the metrics defined in (2.14), (2.15). The rest of the parameters of the signal model and observation model are set to the values defined in Tables 3.1, 3.2. The filters are initalized to the parameter values defined in Table 3.11

Table 3.11: Filter initialization

Parameter	EKF($Q = 0.1^2$)	EKF($Q = 1$)	FPF(50 particles)	FPF(500 particles)
Initial condition	$X_0 = 0$	$X_0 = 0$	$X_0^i \in uniform(0, 2\pi)$	$X_0^i \in uniform(0, 2\pi)$
Model parameter	$a = 2\pi$	$a = 2\pi$	$a^i \in uniform(1.8\pi, 2.2\pi)$	$a^i \in uniform(1.8\pi, 2.2\pi)$
Process noise	$Q = 0.1^2$	$Q = 1$	$\sigma_b^2 = 0.0$	$\sigma_b^2 = 0.0$
Observation noise	$R = 0.1^2$	$R = 0.1^2$	$\sigma_w^2 = 0.1^2$	$\sigma_w^2 = 0.1^2$
	$P_0 = \pi^2/3$	$P_0 = \pi^2/3$	N = 50 particles	N = 500 particles

The process noise covariance σ_b of the signal model is varied from 0.1 to 1.5 in steps of 0.1 and the corresponding error values are calculated for each of the four filters. The following figures Fig. 3.19, Fig. 3.20 show the errors in $\hat{X}_t$ and $\hat{h}_t$ of the filters for the corresponding value of σ_b of the signal model.

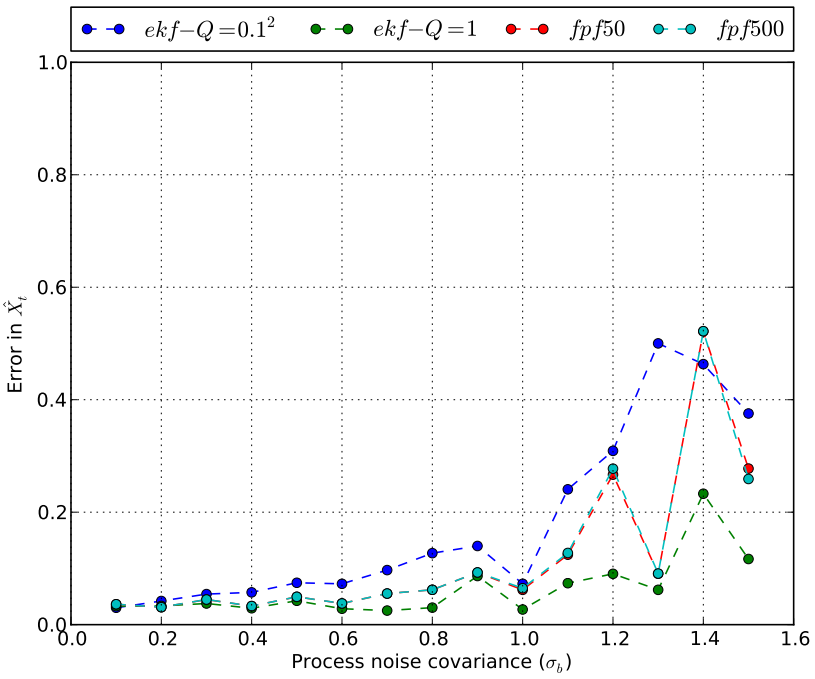

Figure 3.19: X-error vs Process noise covariance(σ_b)

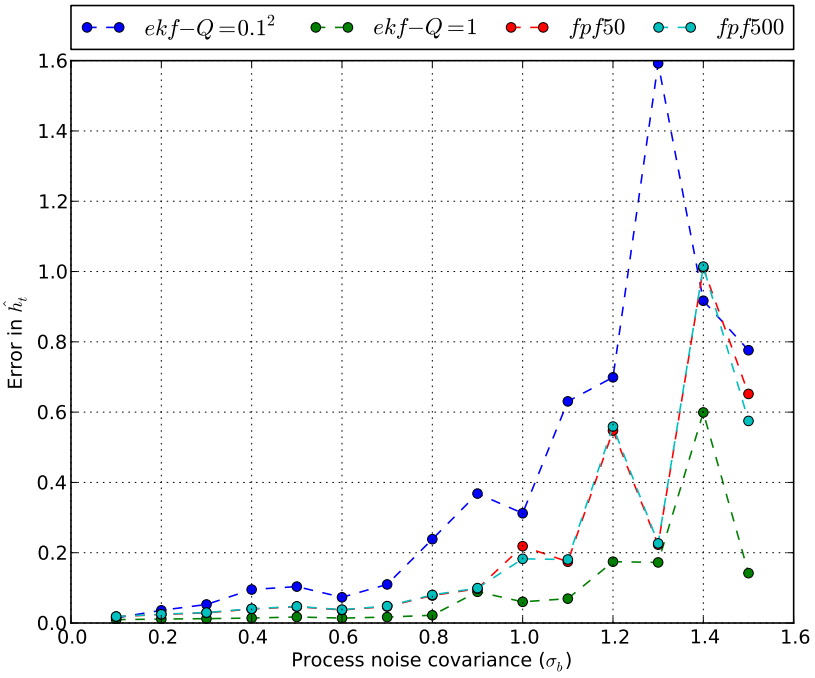

Figure 3.20: h-error vs Process noise covariance(σ_b)

To observe the effects of observation noise of the filters on the performance of

the filters, the above process is repeated for the following two values of observation noise i.e., σ_w of the filters

i. $R = \sigma_w^2 = 0.05^2$ and

ii. $R = \sigma_w^2 = 0.5^2$

i. $R = \sigma_w^2 = 0.05^2$

The filters are intialized to the parameter values defined in Table 3.12. Except for the observation noise (R = σ_w^2) value, all the other parameters are intialized to exactly the same values defined in Table 3.11

Table 3.12: Filter initialization

Parameter	EKF($Q = 0.1^2$)	EKF($Q = 1$)	FPF(50 particles)	FPF(500 particles)
Initial condition	$X_0 = 0$	$X_0 = 0$	$X_0^i \in uniform(0, 2\pi)$	$X_0^i \in uniform(0, 2\pi)$
Model parameter	$a = 2\pi$	$a = 2\pi$	$a^i \in uniform(1.8\pi, 2.2\pi)$	$a^i \in uniform(1.8\pi, 2.2\pi)$
Process noise	$Q = 0.1^2$	$Q = 1$	$\sigma_b^2 = 0.0$	$\sigma_b^2 = 0.0$
Observation noise	$R = 0.05^2$	$R = 0.05^2$	$\sigma_w^2 = 0.05^2$	$\sigma_w^2 = 0.05^2$
	$P_0 = \pi^2/3$	$P_0 = \pi^2/3$	N = 50 particles	N = 500 particles

The process noise covariance σ_b of the signal model is varied from 0.1 to 1.5 in steps of 0.1 and the corresponding error values are calculated for each of the four filters. The following figures Fig. 3.21, Fig. 3.22 show the errors in $\hat{X}_t$ and $\hat{h}_t$ of the filters for the corresponding value of σ_b of the signal model.

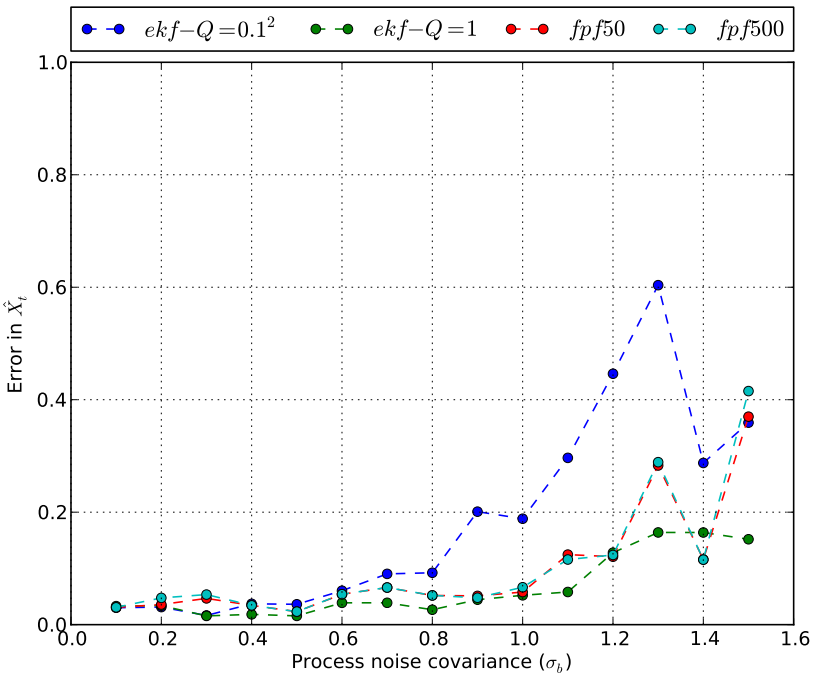

Figure 3.21: X-error vs Process noise covariance(σ_b)

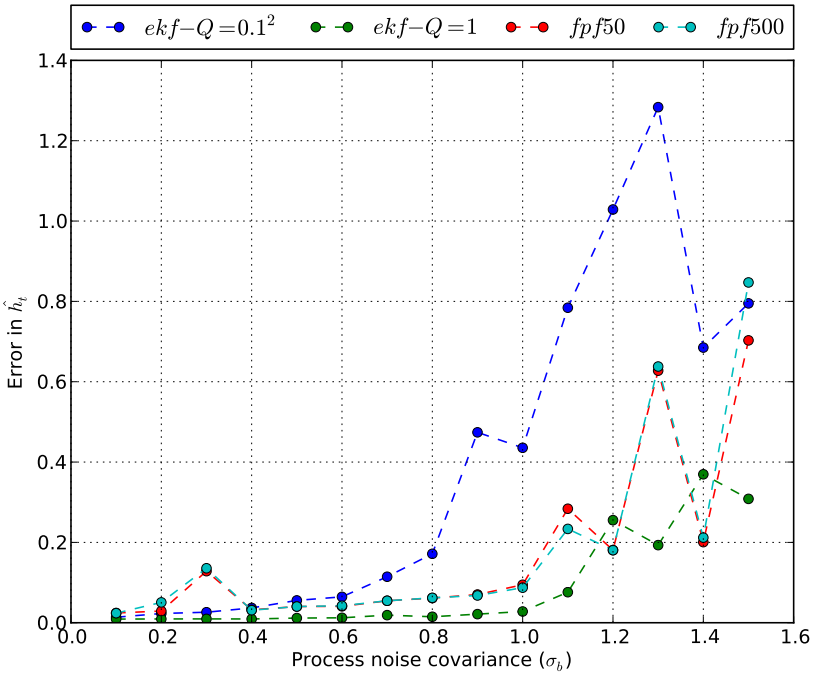

Figure 3.22: h-error vs Process noise covariance(σ_b)

ii. $R = \sigma_w^2 = 0.5^2$

The filters are intialized to the parameter values defined in Table 3.13. Except for the observation noise (R = σ_w^2) value, all the other parameters are intialized to exactly the same values defined in Table 3.11

Table 3.13: Filter initialization

Parameter	EKF($Q = 0.1^2$)	EKF($Q = 1$)	FPF(50 particles)	FPF(500 particles)
Initial condition	$X_0 = 0$	$X_0 = 0$	$X_0^i \in uniform(0, 2\pi)$	$X_0^i \in uniform(0, 2\pi)$
Model parameter	$a = 2\pi$	$a = 2\pi$	$a^i \in uniform(1.8\pi, 2.2\pi)$	$a^i \in uniform(1.8\pi, 2.2\pi)$
Process noise	$Q = 0.1^2$	$Q = 1$	$\sigma_b^2 = 0.0$	$\sigma_b^2 = 0.0$
Observation noise	$R = 0.5^2$	$R = 0.5^2$	$\sigma_w^2 = 0.5^2$	$\sigma_w^2 = 0.5^2$
	$P_0 = \pi^2/3$	$P_0 = \pi^2/3$	N = 50 particles	N = 500 particles

Again the process noise covariance σ_b of the signal model is varied from 0.1 to 1.5 in steps of 0.1 and the corresponding error values are calculated for each of the four filters. The following figures Fig. 3.23, Fig. 3.24 show the errors in $\hat{X}_t$ and $\hat{h}_t$ of the filters for the corresponding value of σ_b of the signal model.

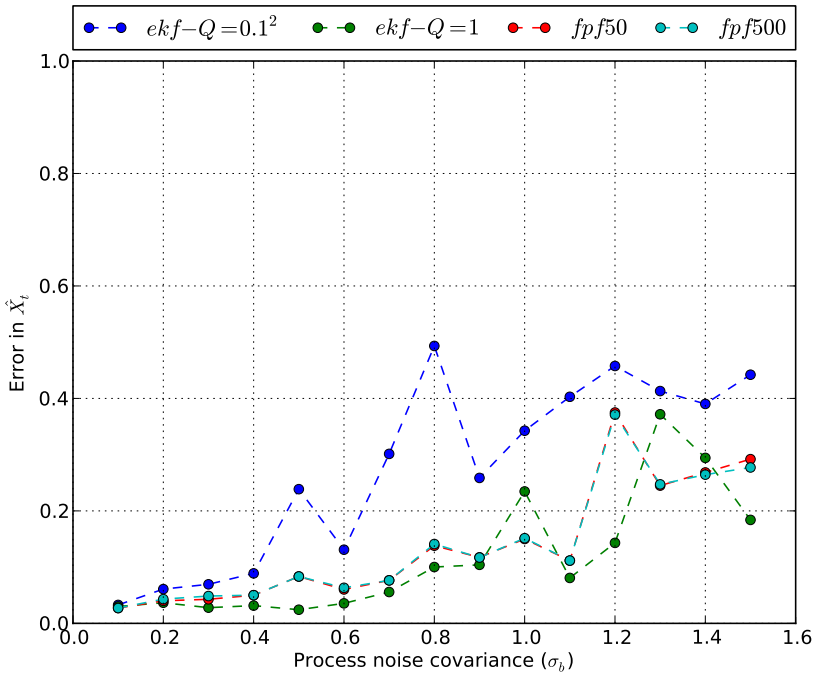

Figure 3.23: X-error vs Process noise covariance(σ_b)

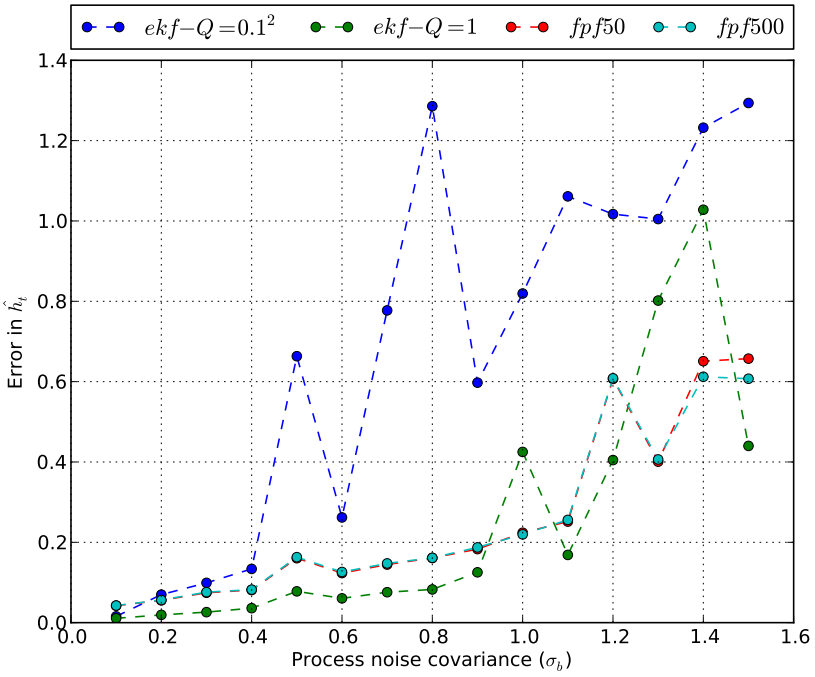

Figure 3.24: h-error vs Process noise covariance(σ_b)

Comparing the three cases against each other, it can be observed that the error values of both $\hat{X}_t$ and $\hat{h}_t$ are lower in the case with lower observation noise of the filter i.e.,$\sigma_w^2 = 0.05^2$ and these values seem to increase slightly with increase in σ_w of the filter. Hence the performance of the filters with respect to the changes in process noise covariance σ_b of the signal model, increased by decreasing the observation noise covariance of the filters.

The case with filter observation noise convariance of $\sigma_w^2 = 0.05^2$, since it has a slightly better performance, is considered to make the following observations:

i. All the four filters were able to cope reasonably well with the small changes in σ_b i.e., $0.1 \leq \sigma_b \leq 0.6$. From the plots it can be observed that both $\hat{X}_t$ and $\hat{h}_t$ error values are small enough when $0.1 \leq \sigma_b \leq 0.6$, which indicates that state estimates from all the four filters are close to the actual state of the signal model. It can also be observed from the plots that for $0.1 \leq \sigma_b \leq 0.6$, the performance of
EKF with $Q = 1 \approx$ FPF with 500 particles $\approx$ FPF with 50 particles $\approx$ EKF with $Q = 0.1^2$

ii. When $0.7 \leq \sigma_b \leq 1.0$, except for the EKF with $Q = 0.1^2$, the other filters

are able to give a good estimate of the state of the signal model, which is evident from the low $\hat{X}_t$ and $\hat{h}_t$ error values. From the error plots, it can be said, in this case, that the performance of
EKF with $Q = 1 >$ FPF with 500 particles $\approx$ FPF with 50 particles $>$ EKF with $Q = 0.1^2$

iii. When there are large changes in σ_b i.e., $\sigma_b > 1.0$, both the $\hat{X}_t$ and $\hat{h}_t$ error values are large for the EKF with $Q = 0.1^2$. Hence the instance of EKF with low process noise covariance cannot cope with large changes in σ_b. Even both the instances of FPF have large $\hat{X}_t$ and $\hat{h}_t$ error values, at higher values σ_b. But EKF with $Q = 0.1$ seems to be doing well even at higher values of σ_b. From the error plots, it can be said that the performance of
EKF with $Q = 1 >$ FPF with 500 particles $\approx$ FPF with 50 particles $>$ EKF with $Q = 0.1^2$

3.3.4 Observation noise σ_w

In this section the observation noise covariance σ_w of the observation model is varied and the accuracy of the state estimate obtained from the filters is compared using the metrics defined in (2.14), (2.15). The rest of the parameters of the signal model and observation model are set to the values defined in Tables 3.1, 3.2. The filters are initalized to the parameter values defined in Table 3.14

Table 3.14: Filter initialization

Parameter	EKF($Q = 0.1^2$)	EKF($Q = 1$)	FPF(50 particles)	FPF(500 particles)
Initial condition	$X_0 = 0$	$X_0 = 0$	$X_0^i \in uniform(0, 2\pi)$	$X_0^i \in uniform(0, 2\pi)$
Model parameter	$a = 2\pi$	$a = 2\pi$	$a^i \in uniform(1.8\pi, 2.2\pi)$	$a^i \in uniform(1.8\pi, 2.2\pi)$
Process noise	$Q = 0.1^2$	$Q = 1$	$\sigma_b^2 = 0.0$	$\sigma_b^2 = 0.0$
Observation noise	$R = 0.1^2$	$R = 0.1^2$	$\sigma_w^2 = 0.1^2$	$\sigma_w^2 = 0.1^2$
	$P_0 = \pi^2/3$	$P_0 = \pi^2/3$	N = 50 particles	N = 500 particles

The observation noise covariance σ_w of the observation model is varied from 0.01 to 0.1 in steps of 0.01 and the corresponding error values are calculated for each of the four filters. The following figures Fig. 3.25, Fig. 3.26 show the errors in $\hat{X}_t$ and $\hat{h}_t$ of the filters for the corresponding value of σ_w of the observation model.

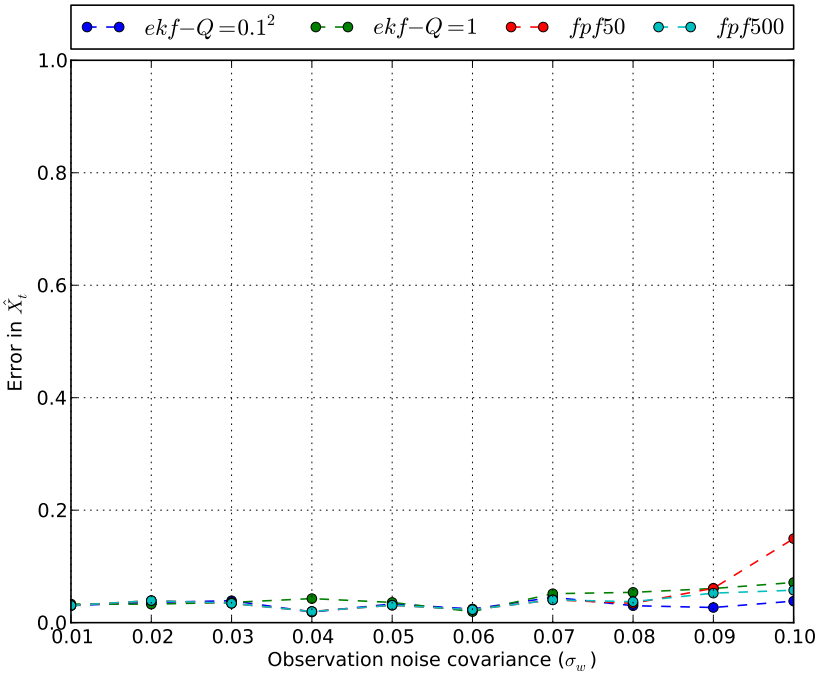

Figure 3.25: X-error vs Observation noise covariance(σ_w)

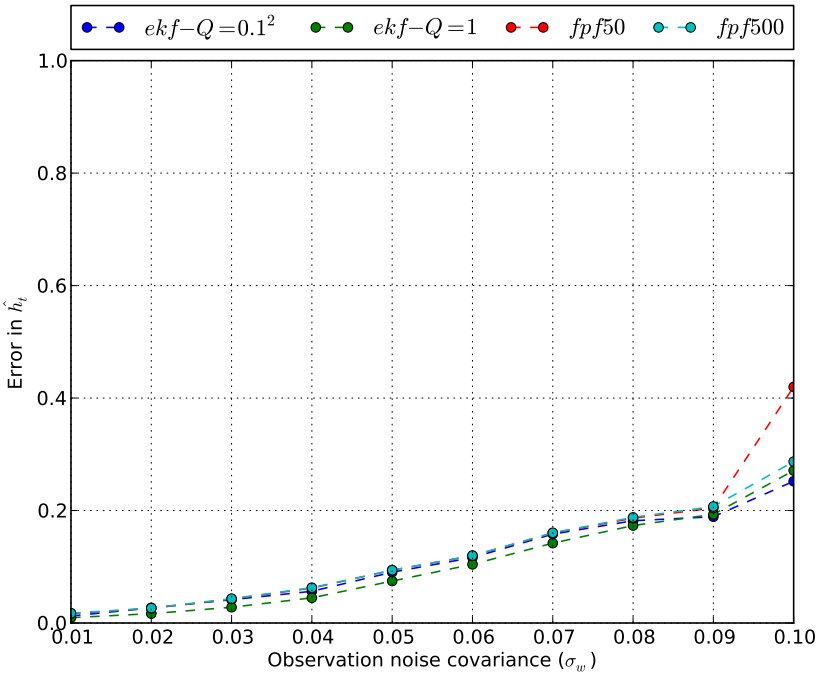

Figure 3.26: h-error vs Observation noise covariance(σ_w)

From the above plots, the following observations can be made:

i. The performance of the four filters based on the error in $\hat{X}_t$ is fairly invariant to the changes in σ_w of the observation model. The $\hat{X}_t$ error values are very low indicating that the state estimates from all the four filters are very close to the actual state of the signal model even with highly noisy observations.

ii. It can also be observed that with an increase in σ_w of the observation model, the $\hat{h}_t$ error values also increase. This is expected because increasing the observation noise messes up the h-functions hence increasing the $\hat{h}_t$ error

3.3.5 Unknown observation model dynamics

The h-function of all the filters is changed to

$$h(x) = 1 + \cos(x) + \sin(x), \tag{3.3}$$

The h-function of the observation model is changed to

$$h(x) = 1 + \cos(x) + \sin(x) + c_2 \cos(2x) + s_2 \sin(2x), \tag{3.4}$$

In this section the h-function of the observation model is varied by changing the coefficients c_2 and s_2 and the accuracy of the state estimate obtained from the filters is compared using the metrics defined in (2.14), (2.15). The rest of the parameters of the signal model and observation model are set to the values defined in Tables 3.1, 3.2. The filters are initalized to the parameter values defined in Table 3.15

Table 3.15: Filter initialization

Parameter	EKF($Q = 0.1^2$)	EKF($Q = 1$)	FPF(50 particles)	FPF(500 particles)
Initial condition	$X_0 = 0$	$X_0 = 0$	$X_0^i \in uniform(0, 2\pi)$	$X_0^i \in uniform(0, 2\pi)$
Model parameter	$a = 2\pi$	$a = 2\pi$	$a^i \in uniform(1.8\pi, 2.2\pi)$	$a^i \in uniform(1.8\pi, 2.2\pi)$
Process noise	$Q = 0.1^2$	$Q = 1$	$\sigma_b^2 = 0.0$	$\sigma_b^2 = 0.0$
Observation noise	$R = 0.1^2$	$R = 0.1^2$	$\sigma_w^2 = 0.1^2$	$\sigma_w^2 = 0.1^2$
	$P_0 = \pi^2/3$	$P_0 = \pi^2/3$	N = 50 particles	N = 500 particles

The coefficients c2 and s2 are varied such that $c = \frac{1}{2}(c_2^2 + s_2^2)$ is varied from 0 to 1 in steps of 0.05 and the corresponding error values are calculated for each of

the four filters. The following figures Fig. 3.27, Fig. 3.28 show the errors in $\hat{X}_t$ and $\hat{h}_t$ of the filters for the corresponding value of $c = \frac{1}{2}(c_2^2 + s_2^2)$ of the observation model.

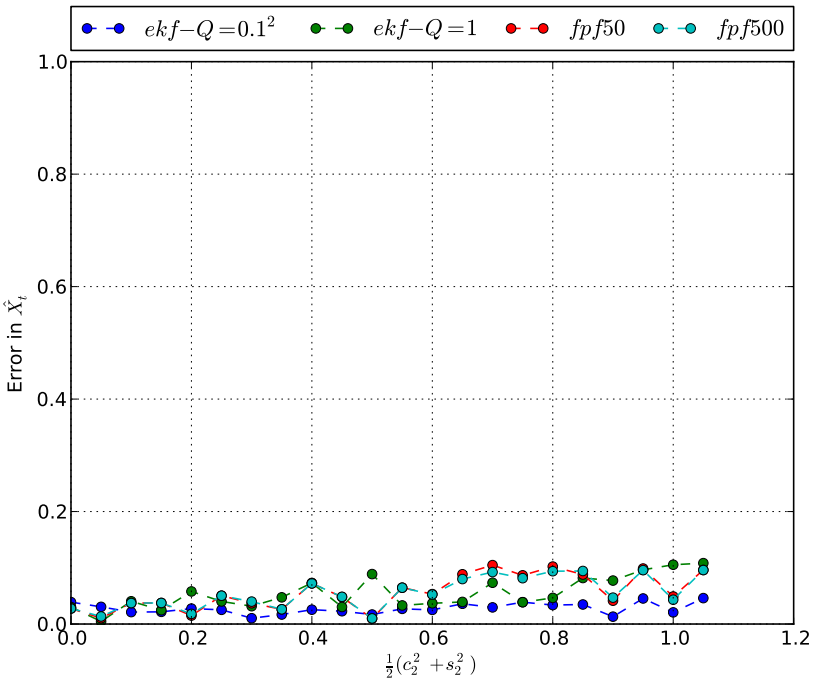

Figure 3.27: X-error vs $c = \frac{1}{2}(c_2^2 + s_2^2)$

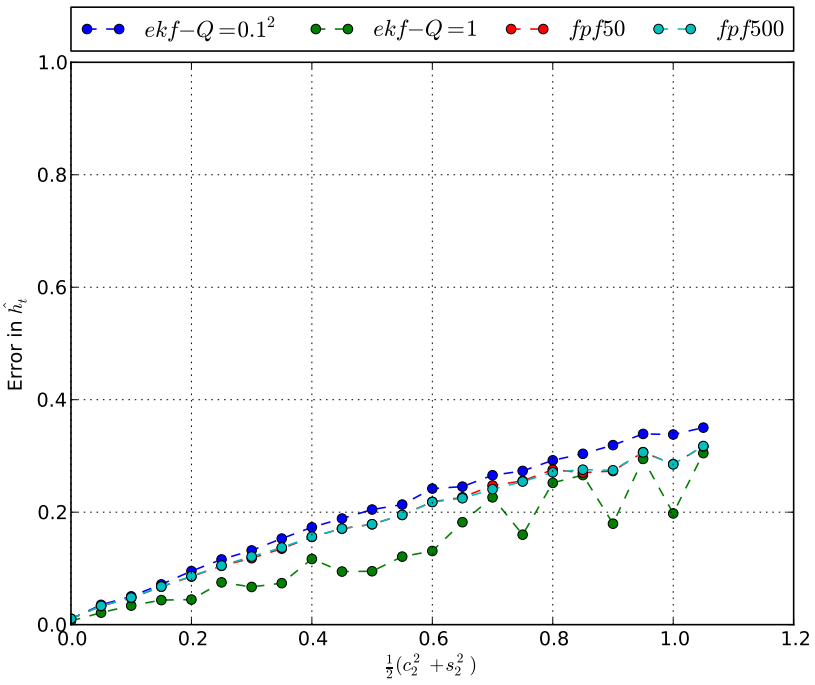

Figure 3.28: h-error vs $c = \frac{1}{2}(c_2^2 + s_2^2)$

From the above plots, the following observations can be made:

i. From the $\hat{h}_t$ error plot, it can be observed that the EKF with $Q = 0.1^2$ has the highest $\hat{h}_t$ error, followed by the two FPF's and then EKF with $Q = 1$. This indicates that the h-function of the EKF with $Q = 1$ is closer to the actual observation model

ii. From the $\hat{X}_t$ error plot, it can be observed that EKF with $Q = 0.1^2$ has the lowest error among the four filters.

REFERENCES

[1] B. Ristic, S. Arulampalam, and N. Gordon. *Beyond the Kalman Filter: Particle Filters for Tracking Applications*. Artech House, Boston, MA, 2004.

[2] A. K. Tilton, T. Yang, H. Yin, and P. G. Mehta. Feedback particle filter-based multiple target tracking using bearing-only measurements. In *Proc. 15th Int. Conf. on Inf. Fusion*, pages 2058–2064, Singapore, July 2012.

[3] T. Yang, H. A. P. Blom, and P. G. Mehta. Interacting multiple model-feedback particle filter for stochastic hybrid systems. In *Submitted to* 52^{nd} *IEEE Conf. Decision and Control*, Firenze, Italy, December 2013.

[4] T. Yang, G. Huang, and P. G. Mehta. Joint probabilistic data association-feedback particle filter for multi-target tracking application. In *Proc. of the 2012 American Control Conference*, pages 820–826, Montréal, Canada, June 2012.

[5] T. Yang, R. S. Laugesen, P. G. Mehta, and S. P. Meyn. Multivariable feedback particle filter. In *Proc. of* 51^{st} *IEEE Conf. Decision and Control*, pages 4063–4070, Maui, HI, Dec 2012.

[6] T. Yang, P. G. Mehta, and S. P. Meyn. Feedback particle filter with mean-field coupling. *In Proc. of IEEE Conference on Decision and Control*, pages 7909–7916, December 2011.

[7] T. Yang, P. G. Mehta, and S. P. Meyn. A mean-field control-oriented approach to particle filtering. *In Proc. of American Control Conference*, pages 2037–2043, June 2011.